Applications of residual stress in combatting fatigue and fracture

JAMES, M Neil, HATTINGH, Danie G, ASQUITH, David <http://orcid.org/0000-0002-0724-7415>, NEWBY, Mark and DOUBELL, Philip

Published version

JAMES, M Neil, HATTINGH, Danie G, ASQUITH, David, NEWBY, Mark and DOUBELL, Philip (2016). Applications of residual stress in combatting fatigue and fracture. Procedia Structural Integrity, 2, 11-25.

Available online at www.sciencedirect.com

ScienceDirect

Procedia Structural Integrity 2 (2016) 011–025

Structural Integrity Procedia

www.elsevier.com/locate/procedia

21st European Conference on Fracture, ECF21, 20-24 June 2016, Catania, Italy

Applications of Residual Stress in Combatting Fatigue and Fracture

M N James [a, b]*, D G Hattingh [b], D Asquith [c], M Newby [d] and P Doubell [d]

[a] *Marine Science & Engineering, University of Plymouth, Plymouth, ENGLAND*
[b] *Mechanical Engineering, Nelson Mandela Metropolitan University, Port Elizabeth, SOUTH AFRICA*
[c] *Engineering and Mathematics, Sheffield Hallam University, Sheffield, ENGLAND*
[d] *Eskom Holdings SOC Ltd, Rosherville, Johannesburg, SOUTH AFRICA*

Abstract

Residual stresses have a significant impact on the propensity for engineering components and structures to undergo fatigue and fracture, with either a positive (life enhancing) or negative (life reducing) effect that is largely dependent on the sign of the residual stress relative to that of the applied stress, i.e. on whether they add to, or subtract from, the applied stresses. Accurate life prediction relies on accurate experimental assessment of residual stresses, often combined with simulation using advanced numerical analysis techniques, that must be calibrated against real service data and this implies a necessity for ongoing condition monitoring. The present paper will outline some industrial applications where detailed knowledge of residual stress is advantageous in assessing their influence on fatigue and fracture performance, and hence assists in combatting failure. It will also draw attention to some examples of failures of expensive structures where residual stresses played a role and consider the design and/or fabrication measures that would have led to an amelioration of the level of residual stress and hence prolonged life.

Peer-review under responsibility of the Scientific Committee of PCF 2016.

Keywords: residual stresses; steam turbine blade and disc; friction taper hydro-pillar processing; weld repair; cracking

1. Introduction

As noted in a number of recent papers, e.g. Withers (2007), James et al. (2007), James (2001), residual stresses have a significant impact on the propensity for engineering components and structures to undergo fatigue and fracture, with either a positive (life enhancing) or negative (life reducing) effect that is largely dependent on the sign of the residual stress relative to that of the applied stress, i.e. on whether they add to, or subtract from, the applied

* Corresponding author. Tel.: +44-1752-586-021; fax: +44-1752-586-103.
E-mail address: mjames@plymouth.ac.uk

Peer review under responsibility of the Scientific Committee of PCF 2016.
10.1016/j.prostr.2016.06.003

stresses. The high level of residual stress induced during most manufacturing operations is often not fully realized by engineering designers (see for example, residual stresses induced during hot [Hidveghy et al. (2003)] and cold [De Giorgi (2011)] rolling), with surface modification and welding techniques being particularly influential in determining fatigue and fracture performance. An additional complexity with predicting the influence of residual stresses on components or structures arises from their potential modification during stress cycling and there is no definitive guidance available to assist with predicting this effect. A classic example of this aspect of stress modification during fatigue cycling is the relaxation of shot peening stresses in the fir tree root region of steam turbine blades during service, which can lead to expensive blade failures [Nwby et al. (2014)]. Shot peening has been used for many years as a means of combatting fatigue failure via mechanical pre-stressing of the surface of engineering parts; Cary (1981) and Guagliano (2011) have both provided interesting reviews of its chronological development.

Nomenclature

ILL	Institut Laue-Langevin, Grenoble, France
ESRF	European Synchrotron Radiation Facility, Grenoble, France
PWHT	Post-weld heat treatment
FTHP	Friction taper hydro-pillar processing
HAZ	Heat-affected zone of a weld
SCC	Stress–corrosion cracking
EDM	Electro-discharge machining

Tensile residual stresses are usually the most detrimental in general service, and, in the presence of a macroscopic notch, they can also lead to fatigue crack initiation and growth during compression-compression fatigue. In these cases, the notch root region undergoes plastic deformation during the compressive fatigue loading and develops a tensile residual stress field during the unloading part of the fatigue cycle. The superimposed compression fatigue loading then leads to tensile fatigue cycling in the plastic zone. An example of a situation where tensile residual stress associated with compression fatigue of a notch can lead to fatigue crack growth is that of hard materials Suresh (1988), where the phenomenon can be useful in pre-cracking of standard fracture toughness specimens, e.g. James et al (1990). Fatigue crack growth under compression-compression loading has been analyzed by Vasudevan and Sadananda (2011) while Lenets (1997) has considered environmentally-assisted compression fatigue of metallic materials [Lenets (1997)]. Examples of this mechanism in action, leading to failure of aircraft landing gear struts and other components, have been reported.

Predicting fatigue performance in the presence of residual stress fields remains complex, particularly for welded structures, although documents such as BS 7910:2013 now provide generalized guidance on residual stress profiles in as-welded joints (annex Q) and on the likely values of residual stress in structures subject to post-weld heat treatment (section 7.1.8.3) in an enclosed furnace with temperature ranges between 550ºC to 620ºC. The guidance further notes, however, that where local post-weld heat treatment is carried out no general recommendations can be given and conservative assumptions should be made; this would be the usual case for welded structures. Stacey et al. (2000) have discussed the incorporation of residual stress assessment procedures into the EU SINTAP defect assessment procedure and note that the SINTAP procedure is built on the guidance contained in BS 7910 and the CEGB R6 procedures. SINTAP is an acronym for Structural Integrity Assessment Procedures, a project funded by the European Community whose aim was to develop a unified procedure for European Industry that covered structural integrity assessment of structures and components.

Accurate life prediction relies on accurate experimental assessment of residual stresses, often combined with simulation using advanced numerical analysis techniques. In recent years, very significant advances have been made in our ability to perform full-field measurements of residual stresses using sophisticated 3D synchrotron X-ray and neutron diffraction techniques, along with automated stages that allow precise location of measurement points coupled with software-driven data analysis. At certain facilities, including the Institut Laue-Langevin (ILL) and the European Synchrotron Radiation Facility (ESRF) in Grenoble, France, it is also possible to apply fatigue loading in-

situ on a beamline whilst making residual stress measurements. For any particular critical engineering application, 3D residual stresses can then be measured at points of local stress concentration and used to calibrate detailed finite element models of complex welded (or other) structures, and hence to produce estimates of fatigue life under the loading conditions of interest. Withers (2007) describes both these nondestructive techniques and other destructive techniques for measuring residual stress in some detail in an excellent review paper.

In engineering service, life prediction exercises must be calibrated against real service data and this implies a necessity for ongoing condition monitoring. The main difficulty here is the large variability among residual stress levels in nominally similar welds and structural geometries (or even rolled members), often arising from relatively minor variations in manufacturing, fabrication, heat treatment or service loading. Condition monitoring in service therefore has to be seen as an integral part of a fracture mechanics-based life assessment for complex structures that is intended to support run-repair-replace decisions. There are stringent requirements stipulated for repair processes on, for example, boilers and pressure vessels, and part of making a case for incorporation of a new repair technique into codes and standards is likely to involve an assessment of the residual stresses induced during repair and their alleviation by post-weld heat treatment (PWHT).

Alongside developments in our ability to measure residual stress fields, significant technological advances in manufacturing capability have also occurred over the last 25 years. One such area of advance is in solid state friction processing techniques, which now have significant applications in, amongst other areas, cost-effective monitoring of creep damage and repair for thermal power plant pipework, discs and blades, e.g. Hattingh et al. (2015). The present paper will outline some industrial applications where detailed knowledge of residual stress is advantageous in assessing their influence on fatigue and fracture performance, and hence assists in combatting failure. It will also draw attention to some examples of failures of expensive structures where residual stresses played a role and consider the design and/or fabrication measures that would have led to an amelioration of the level of residual stress and hence prolonged life. This paper is therefore intended to present a summary of previously published work, some new residual stress results on steam generation components, and several industrial examples of residual stress assisted failure.

2. Power generation applications

2.1. Assessment and repair of steam turbine blade attachment holes

As noted in reference [Hattingh et al. (2015)], turbine failures cost the power generation industry very significant sums of money annually and they generally reflect blade and rotor disc problems. Alongside a desire to reduce these costs, there are strong additional economic pressures to move towards longer intervals between major turbine inspection outages, backed up by risk and decision analysis based on quantitative, sample-based condition monitoring and a probabilistic fracture mechanics-based life assessment. More cost-effective techniques for assessment of creep damage and cracking, where the repair process is also incorporated into the sampling platform, are therefore very attractive to power station owners. Hattingh et al (2015) discussed the deployment of a novel bespoke friction taper hydro-pillar (FTHP) welding technique to repair stress corrosion cracks (SCC) in the central blade attachment prong of a stage 1 LP turbine disc in a 200 MW unit. The innovative FTHP platform (Figure 1) can be mounted on a steam turbine rotor and is capable of performing a sequence of operations that include extracting annular samples from around the attachment prong holes for creep analysis, repairing the hole by FTHP welding and subsequently drilling a new attachment hole. The technique employs the so-called WeldCore® process and the FTHP welding process has now been accepted by ASME for inclusion as an accepted repair technique in Section IX of their Boiler and Pressure Vessel Code (2015). An integral part in the certification of a new repair technique is the assessment of residual stresses and, in work that underpinned deployment of the FTHP process, residual stresses were measured in 5 specimens of DIN 26NiCrMoV14-5 steel representing the various stages in the repair process (see Figure 2). This work was performed at the ILL in Grenoble, France, in experiment 1-02-83 using the SALSA beamline.

In this case, knowledge of the residual stresses is being used to assess the effectiveness of PWHT in reducing peak residual stress values to <100 MPa. This then means that the stresses during service (applied plus residual) will

be close to that applicable to the original attachment hole and the turbine can continue operation with a similar fatigue/SCC performance to that pertaining to the original blade, provided that weld defects are not present. The PWHT involved heating the specimens (each 95 mm x 95 mm x 18 mm) in a furnace at 680ºC for 1 hour followed by furnace cooling. The temperature of 680°C is below the A_{C1} temperature for this steel (725°C; A_{C1} is the austenite transformation start temperature on heating the steel) and the PWHT was therefore intended to achieve stress-relaxation by reducing the yield strength of the material to the level of an acceptable residual stress (<100 MPa). The effectiveness of PWHT is illustrated in Figure 3, which shows the Vickers microhardness profile at three depths in the 18 mm thick W5 specimen (undrilled with PWHT); it is clear that they have been substantially reduced from the peak values of ~500 H_V observed with the as-welded and undrilled specimen (W2). Note that the coordinate axes are defined as *x* and *z* transverse to the hole and *y* is defined through the thickness with zero at the top surface of the specimen. Figure 4 compares the residual stress at three depths in specimen W2 with W5; peak magnitudes are reduced from circa 400 MPa to 500 MPa to <100 MPa. The results also indicated that drilling an 8 mm hole in the as-welded specimen (W3), to simulate a new pin attachment hole, led to a positive residual stress near the free surface in the *x* and *y*-coordinate directions; PWHT (W4) then decreased the magnitude of the residual stress around the hole to < 100 MPa in all three coordinate directions, Hattingh et al. (2015).

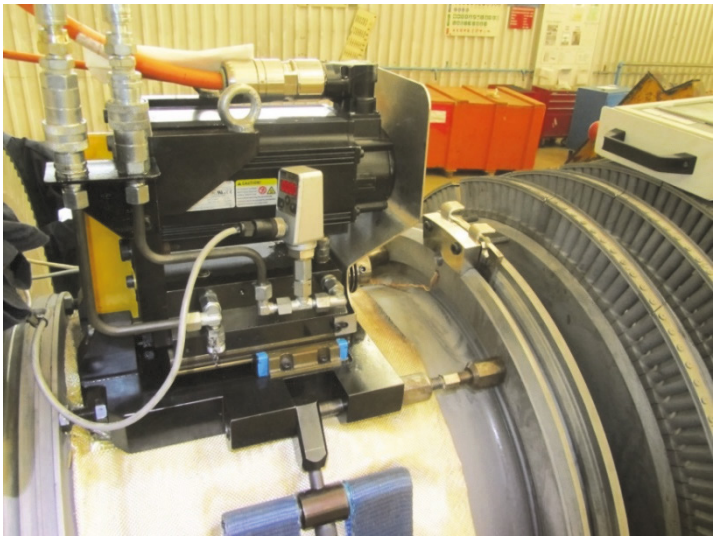

Figure 1. Illustration of the bespoke FTHP platform in position on a stream turbine rotor. It uses the registered WeldCore® process and is capable of extracting an annular metallurgical sample through the thickness of the blade attachment t-slot wall, repairing and re-drilling the hole in a single sequence of operations.

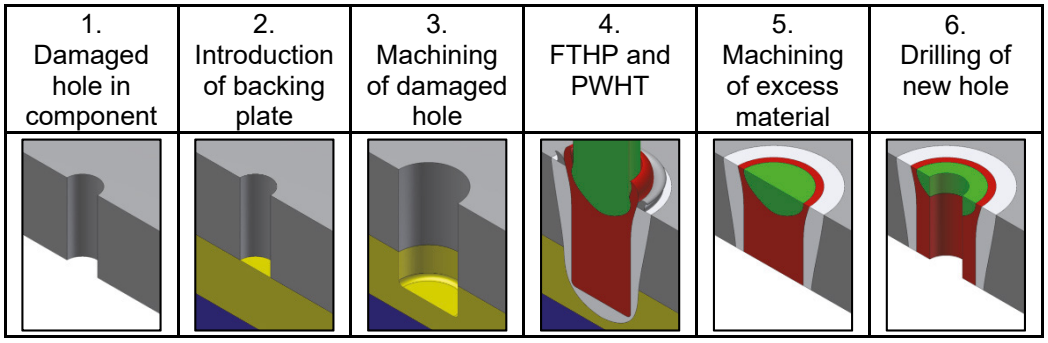

Figure 2. Stages in the FTHP repair of damaged turbine blade attachment finger holes in a LP rotor. Residual stress measurements were made on specimens representing stages 5 and 6 in both the as-welded and PWHT conditions.

2.2. *Damage assessment and repair of thick-walled steam pipe*

Janovec et al. (2012) have discussed the assessment of creep damage and life assessment for BS EN10216 Grade 14MoV6-3 (Material number 1.7715) steam pipes in Czech power plants. They state that in terms of destructive assessment of creep damage "it is necessary to interrupt the operation and remove a part of the steam pipeline". This is clearly a very costly way of performing sampling that provides through-thickness information on creep damage that is not available from either surface replication or 'boat' sampling techniques, Gooch (2003). However, the FTHP process is not restricted to repairing damage at turbine blade attachment holes on LP turbines and can also be used for in-situ creep specimen sampling.

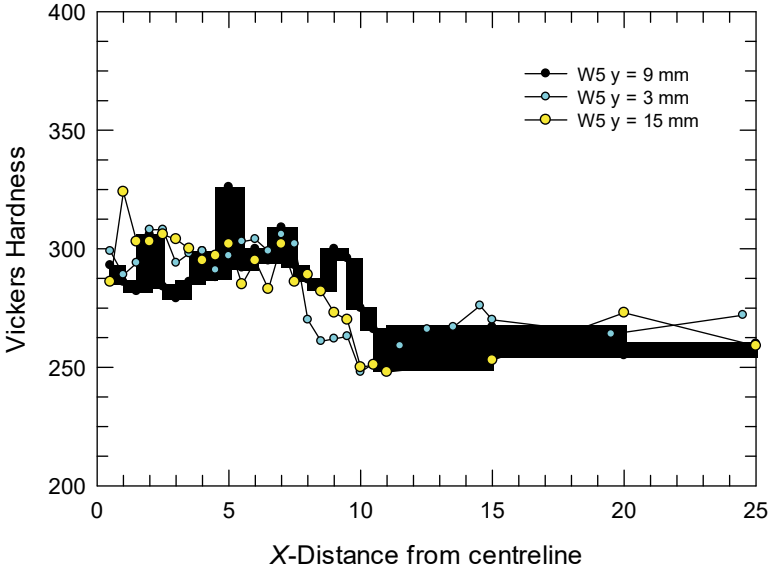

Figure 3. Vickers hardness profiles under a 500gf load in specimen W5 (un-drilled and PWHT) at three depths in the 18 mm thick steel.

In this respect, the present authors have performed trial creep sampling work on 750 mm long sections of thick-walled (42 mm) steam pipe with an outer diameter of 366 mm, manufactured from material 1.7715 grade steel using the WeldCore® technique and a similar bespoke FTHP processing platform to that discussed above. Material 1.7715 is a Cr-Mo-V (Cr 0.30-0.60; Mo 0.50-0.70; V 0.22-0.32) alloy steel used to manufacture seamless pipe for high temperature and pressure service. It typically has a tensile strength R_m in the range 460-610 MPa and a minimum yield strength R_{eH} in the range 300-320 MPa. In Experiment 1-02-128 performed on the SALSA beamline at the ILL in Grenoble, the residual stresses were measured in specimens cut from these steam pipe sections. The aim in this experiment was again to determine the effectiveness of PWHT, in this case using localized induction heating of the steam pipe, after creep sample removal and repair welding of the pipe. High levels of tensile residual stress would be detrimental to the remaining lifetime of the component.

The sequence of events in the WeldCore® creep sampling process is shown in Figure 5 and the FTHP platform is shown in position attached to a piece of steam pipe in Figure 6. In the original planning for this experiment, specimens were prepared from two locations spaced at 90º intervals around the circumference of the pipe. At each position one as-welded specimen and one specimen that had been subjected to localised post-weld induction heat treatment were prepared. In the beamtime available in Experiment 1-02-128 it became necessary to concentrate the residual stress measurement effort on a single as-welded specimen (1A) and on a single specimen (2B) that had been welded and subjected to in-situ PWHT by induction heating (see Figure 7); these specimens were cut from circumferential positions 90º apart and a direct point-based comparison between the residual stresses before and after PWHT is therefore not possible. Nonetheless the residual stresses in the pipe would be expected to be similar

at the two circumferential positions. Full details of the FTHP process are given in Table 1 and the consumable tool was manufactured from BS EN 10216 Grade 10CrMo9-10 (Material number 1.7380). The PWHT was limited to a maximum surface temperature of 800ºC and induction heating was continued until the inner surface of the pipe reached 650ºC which was then maintained for a minimum of 15 minutes. Cooling took place in still air conditions in the laboratory.

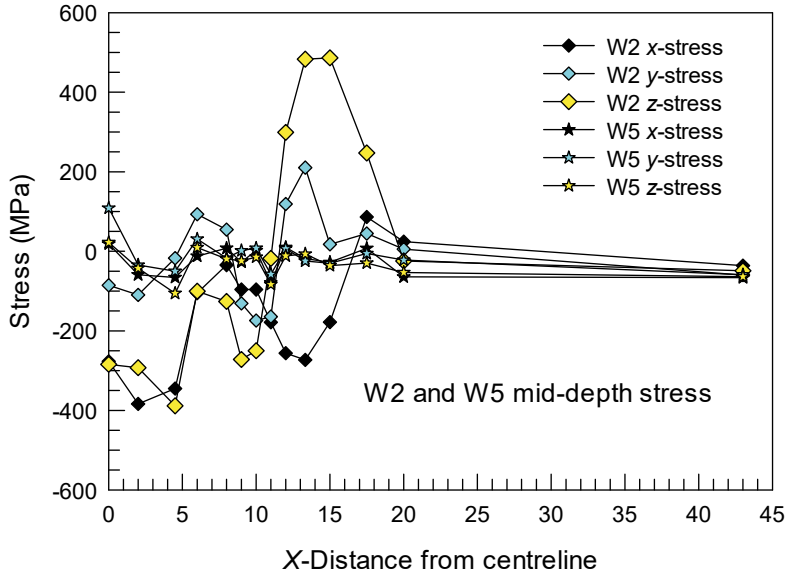

Figure 4. Comparison between the mid-depth values of residual stress in all three coordinate directions for specimens W2 (as-welded and undrilled) and W5. The edge of the original hole in the blade would have been at the x = 4 mm position.

Table 1. Details of the FTHP process.

Pin Taper	Pin Length mm	Pin End mm	Tool Speed rpm	Forging Force kN	Forging Time s
15º	47.5	9	5,000	27	20

Measurements were made of the residual stresses in the hoop, radial and axial directions of the pipe at three positions through the wall thickness (18 mm, 27 mm and 37 mm from the outer surface) at a number of positions between +60 mm and -60 mm from the centreline of the hole. Excellent agreement was observed between stresses at similar positive and negative distances from the centreline. Figure 8 shows the measured residual hoop stresses in specimen 1A (as-welded – Figure 8a) and specimen 2B (PWHT – Figure 8b) and Figure 9 shows the equivalent (corresponding??) data in the axial direction. In terms of crack initiation during service, these are the two key coordinate directions. Measurements were able to be made at 5 depths in the PWHT specimen, while data was obtained only at three depths in the as-welded specimen.

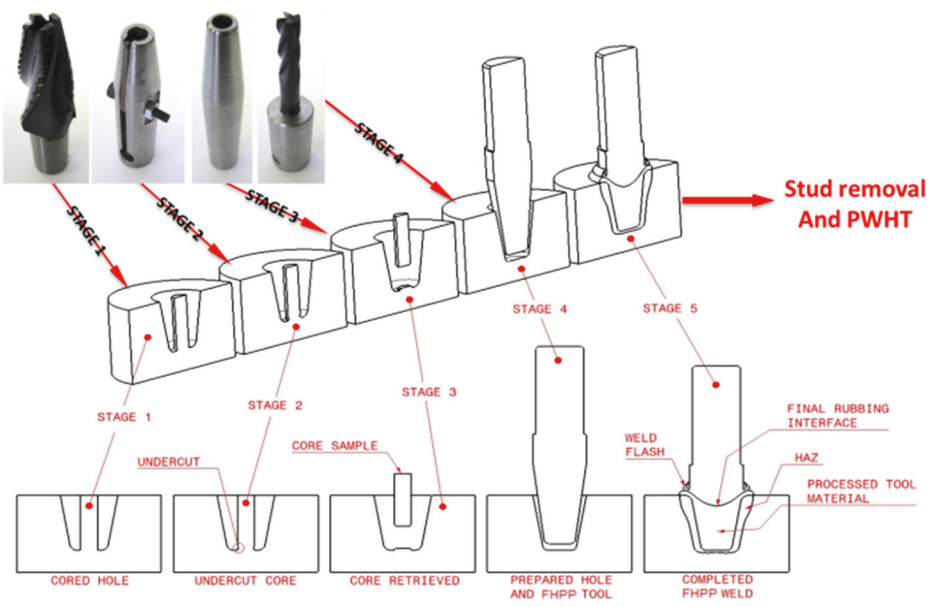

Figure 5. Sequence of events that occur in the WeldCore® process using a bespoke FTHP processing platform.

Figure 6. FTHP processing platform in-situ on a section of thick walled steam pipe. The pads are for preheating the pipe to approximately 200ºC prior to commencing the WeldCore® process.

Figure 7. Induction heat treatment of the pipe after completion of the WeldCore® process.

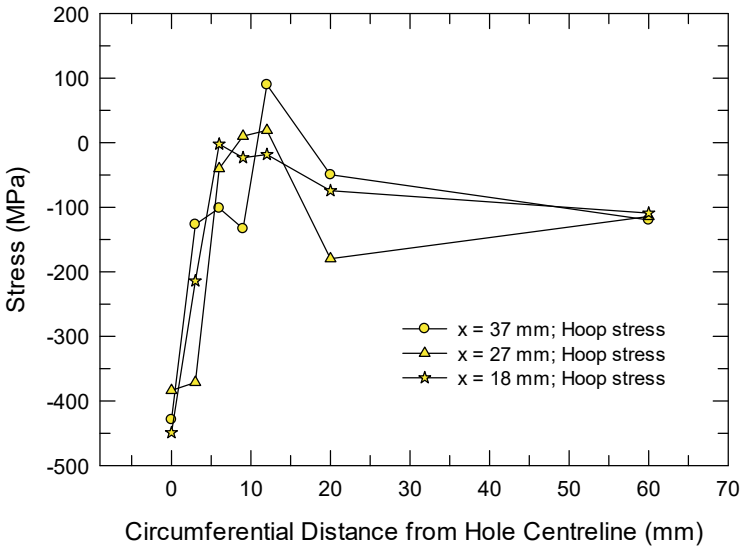

Figure 8a. Residual hoop stresses in the as-welded FTHP specimen 1A.

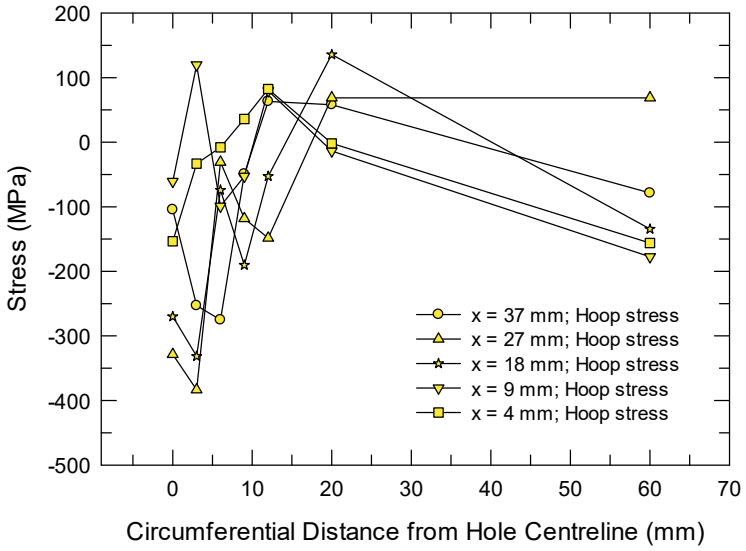

Figure 8b. Residual hoop stresses in specimen 2B after local PWHT by inductive coil.

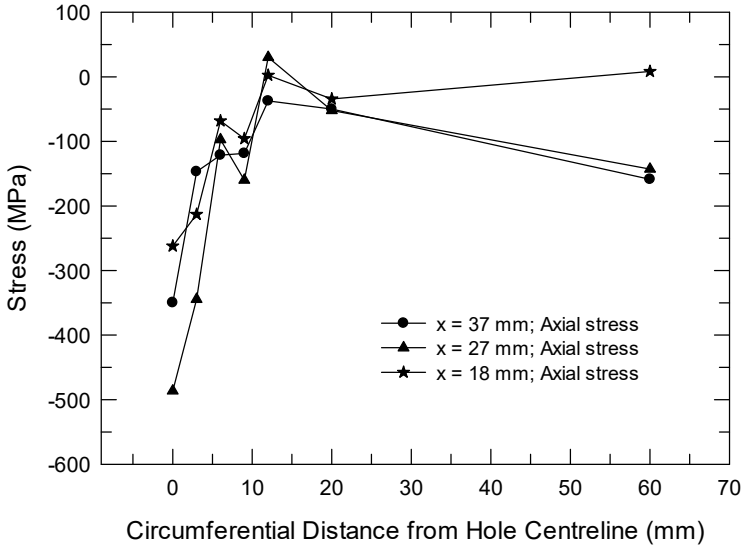

Figure 9a. Residual axial stresses in the as-welded FTHP specimen 1A.

Nonetheless, certain observations can be made from these hoop stress data; firstly, that at depths of 18 mm, 27 mm and 37 mm below the surface of the pipe, the large negative peaks that occur around the edge of the weld metal are reduced from peak values of 380 MPa to 450 MPa in the as-welded state, to values of around 275 MPa to 380 MPa. Secondly, the values of peak tensile hoop stress are also reduced at equivalent depths and, thirdly, the stress distribution moves in the tensile direction the closer to the outer surface the measurements are made (e.g. Figure 8b,

x = 9 mm and x = 4 mm). In all cases where data was obtained, the level of peak tensile hoop residual stress is < 120 MPa.

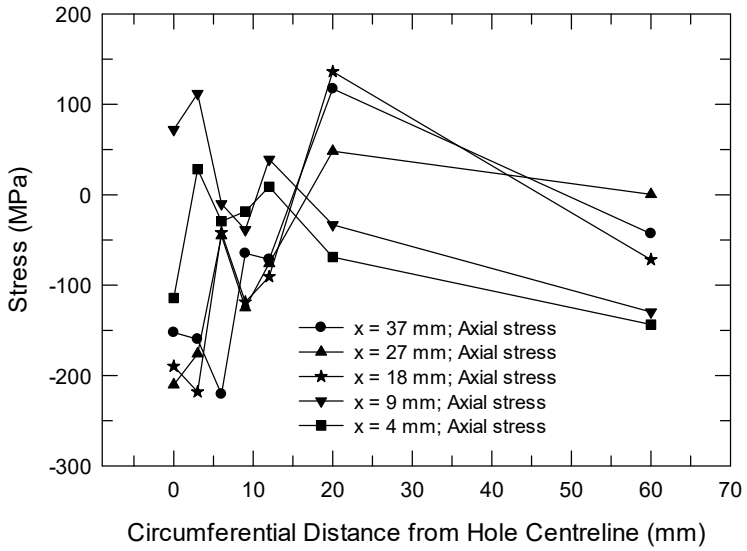

Figure 9b. Residual axial stresses in specimen 2B after local PWHT by inductive coil.

The same general observations are true of the axial stress measurements, although there is a significant difference in that the PWHT appears to sharply increase the stress variation across the heat-affected zone (HAZ) of the weld, between distances of 9 mm and 20 mm from the weld centreline. Peak values of tensile axial stress in all cases are < 140 MPa. Although experimental difficulties led to a smaller set of residual stress measurements than had been planned, it is clear that the FTHP technique can be usefully employed for in-situ through-thickness creep sampling and that the level of tensile residual stress in the pipe wall is < 50% of the lower yield strength of the steel. Localised PWHT reduces the peak negative stresses by some 16% in the hoop direction in the pipe and by up to 38% in the axial direction.

2.3. Residual stresses in turbine blade shroud tenons after laser weld build-up

Tenons on turbine blades are used to position and fix the tips of adjacent blades using a shroud. The function of the shroud is to control the in-service vibration response of the blades. A large number of turbine blades have to be scrapped during turbine maintenance because their tenons have to be ground down to remove the blades for inspection or other maintenance activities. Typically, the estimated replacement cost of a row of blades is €60,000; and although in some cases only single blades have to be replaced, this still requires a number of adjacent blades to be scrapped in order to replace the damaged blade. Blades removed from the disc cannot be re-used as the remaining tenon stub is too short to be riveted to the shroud a second time. Figure 10 shows the blade tenon configuration and illustrates the problem that arises from tenon grinding to remove the shroud.

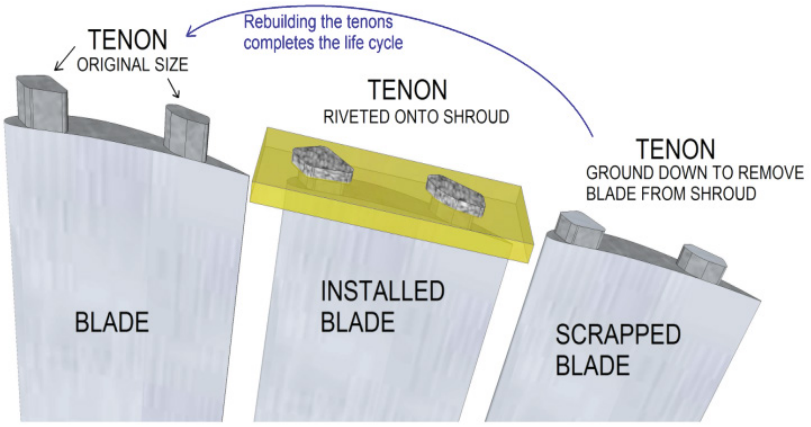

Figure 10. Schematic illustration of the tenon rebuild issue.

Rebuilding tenons by welding is a viable option to repair the blades for further use and there is a strong incentive to implement this procedure is service. However, tenons are subjected to high centrifugal loading during normal service operation at 3,000 rpm and it is well known that the main blade failure mechanisms are SCC, hydrogen-assisted cracking or fatigue, all of which are exacerbated by high levels of tensile residual stress. These turbine blades are manufactured from 12% chromium martensitic stainless steel to material number 1.4939 (trade name Jethete M152). Typical mechanical properties of this material are a measured 0.2% proof stress of 868 MPa and a tensile strength of 1048 MPa; it is known to be prone to stress corrosion and hydrogen induced cracking when subjected to high localised stresses in a susceptible environment. It is therefore important to assess the level of weld residual stresses introduced by candidate weld repair processes, as an integral part of the risk assessment of the refurbishment technique.

This paper reports the residual stress data measured on the SALSA beamline at the ILL, Grenoble in Experiment 1-02-152 for simulated blade specimens in the as-welded and PWHT conditions. This experiment aimed to establish the level and orientation of residual strain introduced to a low pressure steam turbine blade following a weld build-up. The specimen used to simulate the built-up, un-machined tenon is shown in Figure 11. Laser welding was performed at the National Laser Centre of the CSIR, South Africa, using a 3kW IPG YLS-3000-TR power source with the welding head integrated with a KUKA KR60L30 robotic system positioner.

The full experimental matrix involved weld build-up using with either Nickel-based powder (type Inconel 625) or Grade FV520 martensitic stainless steel powder on rectangular coupons machined from Grade FV520B martensitic stainless steel turbine blades whilst maintaining a preheat of 200ºC. Residual stress data was measured in three orthogonal directions at an array of points down the centreline (in both the T and ST directions) of the tenon repair specimens. In this Experiment (1-02-152) and in 1-02-83, the unstrained lattice spacing was measured using toothcomb specimens electrodischarge machined (EDM) from the same material as the residual stress specimens, Hughes et al. (2003). It should be noted that cubes are better than toothcomb specimens to measure the strain-free lattice spacing, unless allowance is made for the macro-stress along the tooth [Ganguly et al. (2011)], which was done in these cases. In the case of Experiment 1-02-128 cubes were produced by EDM and used to make strain-free lattice spacing measurements.

In this paper, we present only the residual stress data obtained from two specimens where the weld consumable used in the repair process was the Grade FV520 martensitic stainless steel powder. The weld build-up was applied in 0.4 mm layers with beads 2 mm wide and 1 mm ‘step-over’ between beads with a heat input of 50.9 kJ/mm. The interpass temperature was maintained at 154°C and the shielding gas was argon. PWHT involved heating at 100°C/hour up to 650°C, holding this temperature for an hour then cooling at 100°C/hour.

Residual stresses were measured in two specimens conditions representing as-welded and PWHT tenon build-up

cases, and the resulting 3D residual stress data are shown in Figure 12a (as-welded) and Figure 12b (PWHT). The zero point for the *x*-axis of Figure 12 is the bottom surface of the test coupon, so the original fusion boundary is at *x* = 45 mm. It is clear that a substantial level of triaxial tensile stress exists on either side of the fusion boundary with peak values of circa 600 MPa. At the fusion boundary the peak stresses have reduced in value with the values in the T and ST directions tending to be negative, while the longitudinal stress remains tensile. It is clear that turbine blade tenons would have a significant risk of experiencing SCC, hydrogen-assisted cracking or fatigue.

In contrast after PWHT, the residual stress peaks are more localised to the fusion boundary transition and the peak tensile values are reduced to 100 – 120 MPa. A small region (≈ 2 mm wide) of triaxial tension still remains associated with the fusion boundary zone.

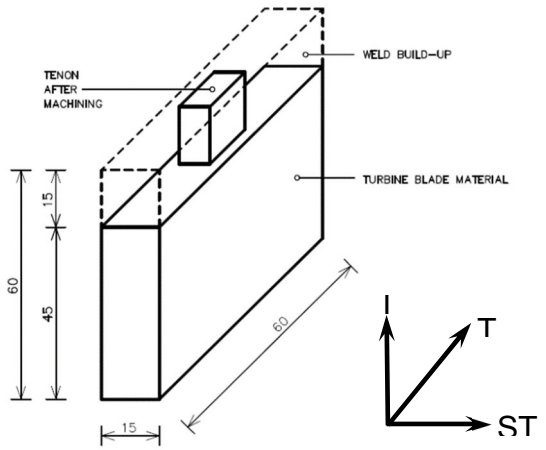

Figure 11. Geometry of the DIN 1.4939 coupon used to simulate tenon build-up by laser welding. The three orthogonal directions for residual stress measurement are longitudinal (L), transverse (T) and short-transverse or through-thickness (ST).

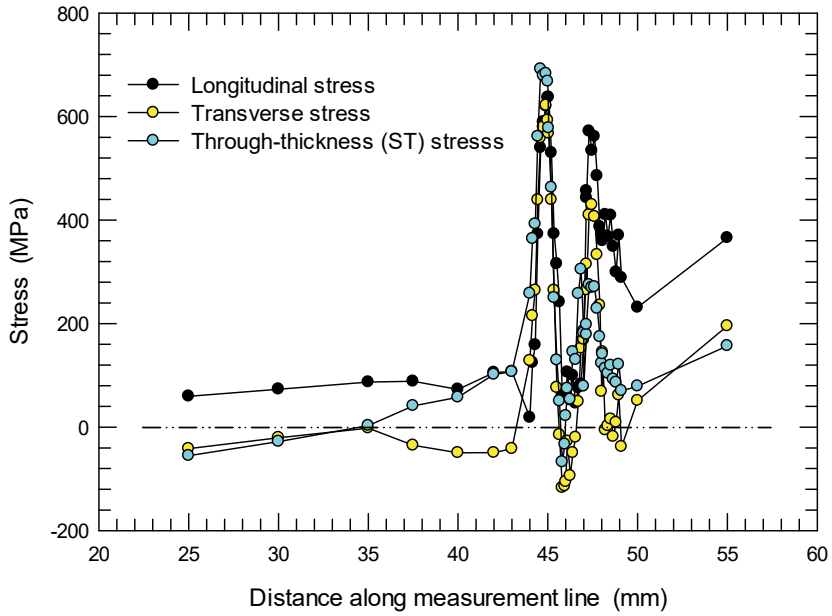

Figure 12a. Residual stress data measured in the as-welded tenon sample.

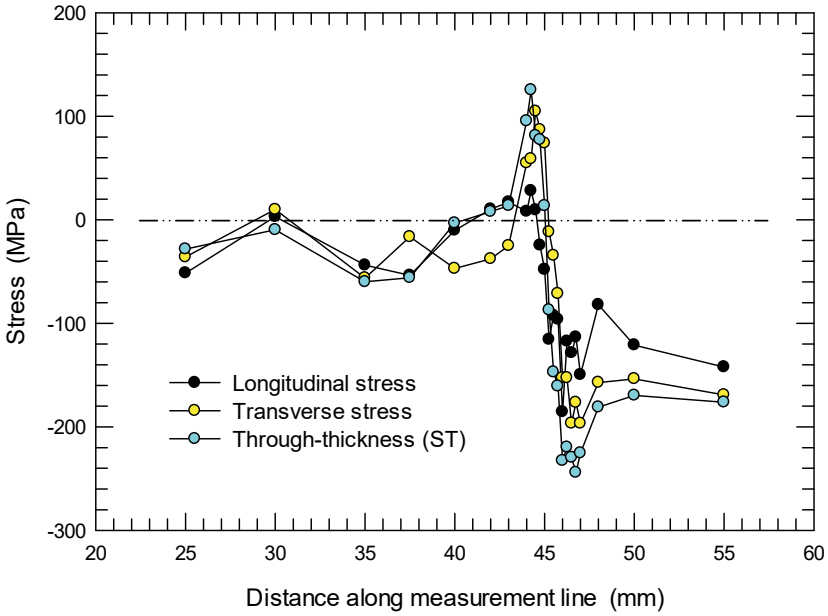

Figure 12b. Residual stress data measured in the PWHT tenon sample.

It can be concluded from this experiment that laser welding refurbishment of the tenons on FV520 martensitic steam turbine blades, coupled with a PWHT process offers a cost-effective way of repairing blades after shroud removal during turbine maintenance.

3. Typical industrial residual stress problem areas

In this final part of the paper, the issue of "learning from history" is introduced through consideration of three fairly straightforward examples of industrial cracking problems arising from design and welded construction, i.e. associated with residual stresses and local stress concentrating features, that could readily have been foreseen as likely to lead to fatigue problems. Some areas of structural design where residual stresses can cause problems which may be overlooked by designers have been covered in references [James et al. (2007), James (2011)]: these include machining of castings where the associated redistribution of residual stress can lead to shape changes and cracking problems, e.g. from fretting fatigue; various types of embrittlement; and changes in the buckling resistance of columns or shell structures that can arise from uneven cooling of hot-rolled structures, or from the earlier onset of plastic deformation with a loss of stiffness in some parts of the strucutral member. Localised stiffness changes are excellent stress concentrating features and are often implicated in failure, even in the absence of an associated residual stress field. Figure 13a shows an example of cracking in a large 14 foot diameter cast girth gear used to rotate a ball mill, where the crack has initiated from a 'metallurgical notch', i.e. a large localised hardness difference arising from a weld upgrade to the casting in the root region of the gear tooth profile (yellow arrow) rather than at the larger region of porosity indicated with the white arrow. Figure 13b shows the associated hardness values and demonstrates a sharp change in hardness in this region of circa 100 H_V.

The final example of a structural cracking problem arising from localised stiffness changes and high levels of residual stress due to incorrect welding procedures concerns the incorporation of knives on the inside of a long, large diameter and relatively flexible cylinder that formed the body of a rotating industrial composter for household waste. The knives were intended to break up bags of rubbish on entry into the composter (a relatively low stress part of the design), but were extended further into the more highly stressed interior for reasons that remain unclear.

The shell alloy was specified as Grade 250 steel (minimum yield strength < 500 MPa) and the knives were specified to be cut from a wear resisting alloy with a proof strength of approximately 1070 MPa. The knives were welded to a backing plate (also specified as Grade 250 steel) which was then welded to the shell. In practice, the knives were manufactured from a higher grade alloy with a yield strength of 1200 MPa and and the backing plate was made from the same alloy.

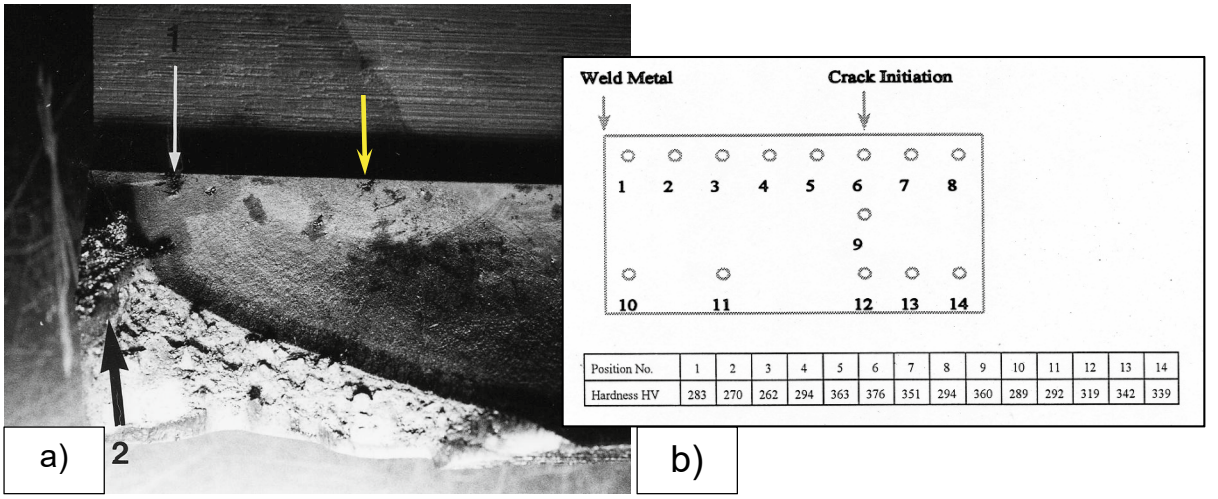

Position No.	1	2	3	4	5	6	7	8	9	10	11	12	13	14
Hardness HV	283	270	262	294	363	376	351	294	360	289	292	319	342	339

Figure 13. Example of cracking in a large cast girth gear caused by a weld upgrade region; a) The crack has initiated at a small region of porosity (yellow arrow) arising from a 100 H_V difference in this region b), rather than from the much larger region of porosity indicated with the white arrow.

It was not clear that the specified welding procedure was developed for this alloy and the net result was a large stress concentration arising from the high local stiffness associated with these knives in an otherwise rather flexible shell (whose flexibility additionally induced two stress cycles in each revolution rather than the single cycle that was included in the fatigue design), combined with high residual stress and hardness levels sufficient to lead to hot cracking and hydrogen cracking at these welds as a result of an incorrect and poorly controlled welding procedures. The design life had ben specified as 20 years and within 9 months of service entry

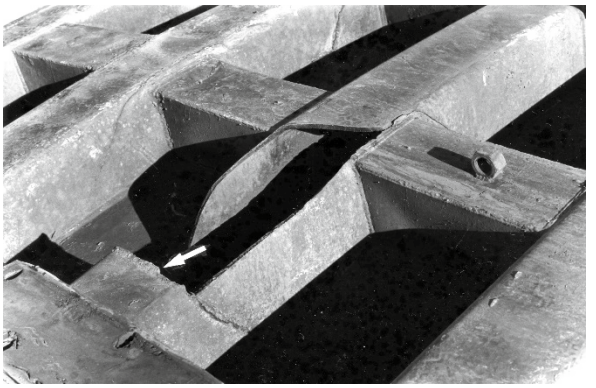

Figure 14. Extensive fatigue cracking observed in a 170 tonne dump truck pan.

4. Conclusions

This paper has presented three examples drawn from the power generation industry and, in particular, related to cost-effective repair of steam turbine blades and discs, intended to illustrate how detailed 3D measurements of residual stresses are an essential part of a structured approach to combatting fatigue and fracture. Facilities such as those at the ILL and the ESRF in Grenoble, France offer a very significant capability in assessing 3D residual stress distributions in substantial pieces of engineering hardware (up to circa 500 kg mass) with 10 μm precision, relatively fast acquisition times and automated analysis of diffraction peaks. Such high resolution data can be coupled with finite element analysis to predict residual stress distributions in components and structures under different conditions and to make predictions of fatigue life [Newby et al. (2014)].

The final part of the paper has illustrated the type of problem that can arise with large and very expensive components and structures when the potential implications of residual stresses are not recognised, and the design process does not actively seek to combat fatigue and fracture. It is hoped that this short overview of the type of data that can be acquired from industrial components and its value in life prediction will be of interest to readers of the journal.

Acknowledgements

The award of beamtime on the SALSA instrument at the Institut Laue-Langevin, Grenoble through experiments 1-02-83, 1-02-128 and 1-02-152, together with the support of the beamline scientist, Dr Thilo Pirling, are gratefully acknowledged.

References

Withers, P.J., 2007. Residual stress and its role in failure. Reports on Progress in Physics, 70(12), 2211-2264.
James, M.N., et al., 2007. Residual stresses and fatigue performance. Engineering Failure Analysis 14(2), 384-395.
James, M.N., 2011. Residual stress influences on structural reliability. Engineering Failure Analysis 18(8), 1909-1920.
Hidveghy, J., Michel, J. N., Bursak, M., 2003. Residual stress in microalloyed steel sheet. Metalurgija 42(2), 103-106.
De Giorgi, M., 2011. Residual stress evolution in cold-rolled steels. International Journal of Fatigue 33(3), 507-512.
Newby, M., James, M.N., Hattingh, D.G., 2014. Finite element modelling of residual stresses in shot-peened steam turbine blades. Fatigue & Fracture of Engineering Materials & Structures 37(7), 707-716.
Cary, P.E., 1981. History of Shot Peening. in 1st International Conference on Shot Peening, Paris, France.
Guagliano, M., 2011. Perspectives and problems in shot peening, a mechanical treatment to improve the fatigue behaviour of structural parts. Anales de Mecánica de la Fractura 28(1), 9-19.
Suresh, S., 1988. The failure of hard materials in cyclic compression: Theory, experiments and applications. Materials Science and Engineering: A 105–106, 323-329.
James, M.N., Human, A.M., Luyckx, S., 1990. Fracture toughness testing of hard metals using compression-compression precracking. Journal of Materials Science 25(11), 4810-4814.
Vasudevan, A.K., Sadananda, K., 2001. Analysis of fatigue crack growth under compression–compression loading. International Journal of Fatigue, 23, 365-374.
Lenets, Y.N., 1997. Compression fatigue crack growth behavior of metallic alloys: Effect of environment. Engineering Fracture Mechanics 57(5), 527-539.
Hsu, T.-Y.J., 2015. Investigation of Cyclic Deformation and Fatigue of Polycrystalline Cu under Pure Compression Cyclic Loading Conditions, in Department of Materials Science. University of Toronto: Toronto. pp. 198.
Stacey, A., et al., 2000. Incorporation of residual stresses into the SINTAP defect assessment procedure. Engineering Fracture Mechanics 67(6), 573-611.
Hattingh, D.G., et al., 2015. Damage assessment and refurbishment of steam turbine blade/rotor attachment holes. Theoretical and Applied Fracture Mechanics.
ASME, ASME Boiler & Pressure Vessel Code Supplement 3, in Section IX: Welding, Brazing and Fusing Qualifications. 2015, American Society of Mechanical Engineers: New York, USA.
Janovec, J., Polachova, D., Junek, M., 2012. Lifetime assessment of a steam turbine. Acta Polytechnica 52(4), 74-79.
Gooch, D.J., 2003. 5.07 - Remnant Creep Life Prediction in Ferritic Materials A2 - Karihaloo, B., Milne, I. and Ritchie, R.O., in Comprehensive Structural Integrity. Pergamon: Oxford. p. 309-359.
Hughes, D.J., et al., 2003.The Use of Combs for Evaluation of Strain-free References for Residual Strain Measurements by Neutron and Synchrotron X-ray Diffraction. Journal of Neutron Research 11(4), 289-293.
Ganguly, S., Edwards, L., Fitzpatrick, M.E., 2011. Problems in using a comb sample as a stress-free reference for the determination of welding residual stress by diffraction. Materials Science and Engineering: A 528(3), 1226-1232.